Sensitivity Enhancement of SPR Sensor Based on $Ti_3C_2T_x$ (MXene) with Composite Layers of TiO_2-SiO_2

Rajeev Kumar, Maneesh Kumar Singh, Sarika Pal, Narendra Pal, and Y. K. Prajapati

Abstract In this seminal, the surface plasmon resonance sensor (SPR) sensor based on $Ti_3C_2T_x$ (MXene) with a composite layer of TiO_2-SiO_2 is theoretically presented. The $Ti_3C_2T_x$ as biomolecular recognition element (BRE) layer enhances the sensitivity of the proposed sensor. The other two important parameter such as detection accuracy (DA) and figure of merit (FoM) have been also deliberated. Firstly, the thicknesses of TiO_2 and SiO_2 are optimized with a monolayer of gold and $Ti_3C_2T_x$ layers for calculation of the sensitivity. The maximum sensitivity achieved is 276°/RIU. The variation in the sensitivity, Rmin, DA, and FoM w.r.t the RI of the sensing medium, is also analyzed. To evaluate the penetration depth for the proposed sensor, we have evaluated the transverse electromagnetic field distribution too. The penetration depth of 197 nm is obtained for the proposed SPR sensor.

Keywords Detection accuracy · Electromagnetic field distribution · FoM · Sensitivity · Sensor · Surface plasmon resonance

R. Kumar · M. K. Singh (✉) · S. Pal
Department of ECE, National Institute of Technology Uttarakhand, Pauri Garhwal, Srinagar 246174, Uttarakhand, India
e-mail: maneeshsingh.phd19@nituk.ac.in

R. Kumar
e-mail: rajeevkumar.phd2020@nituk.ac.in

S. Pal
e-mail: sarikapal@nituk.ac.in

N. Pal
Department of ECE, Rajkiya Engineering College, Kannauj 209732, U.P., India

Y. K. Prajapati
Department of ECE, Motilal Nehru National Institute of Technology Allahabad, Paryagraj 211004, U.P., India
e-mail: yogendrapra@mnnit.ac.in

A. Dhawan et al. (eds.), *Advances in VLSI, Communication, and Signal Processing*, Lecture Notes in Electrical Engineering 911,
https://doi.org/10.1007/978-981-19-2631-0_40

1 Introduction

In biomedical field, a number of biosensors have been developed based on PCR [1], ellipsometry [2], quartz crystal microbalance [3], electrochemistry [4], piezoelectric, spectroscopy, interferometry, colorimetry [5], fluorescence resonance energy transfer [6], surface plasmon resonance, etc. Among the various methods, optical biosensor has attracted the attention of researchers. Surface plasmon resonance (SPR) technique among optical biosensors is a powerful tools for the detection and investigation of DNA hybridization, protein, antigen [7], and virus [8] in real-time with high sensitivity and high-speed response [9]. In a specific application such as detection of DNA hybridization [9, 10], miRNA [11], SPR biosensor has attracted the attention of researchers because of their attractive sensing capability, compactness, robustness, high precision, and reliability. The most widely used SPR biosensor works on the principle of attenuated total reflection (ATR). Surface plasmon polaritons (SPPs) are electron density wave (collective oscillation of free electron gas density) propagating along the interface of dielectric (positive permittivity) and metal (negative permittivity) [12]. Surface plasmon resonance phenomenon achieved when evanescent wave vector of transverse magnetic (TM) polarized light matches with wave vector of SPP wave [13]. At resonance condition, dip in the reflection intensity is observed at SPR angle [14]. Various methods are proposed to improve or enhance the sensitivity of biosensors such as a colloidal gold nanoparticle, nano slits, bimetallic SPR active metal, hybrid layer structure, and 2D material [11]. 2D materials open a new window for researchers working in the field of material science, optoelectronics, and biosensing [15].

Numeral emerging 2D materials such as graphene, black phosphorous (BP), transition dichalcogenides (TMDCs), metal oxides and antimonene has attracted significant interest due to their electrical, and optical properties to enhance the sensitivity of biosensors [16]. Most of the 2D material has certain drawbacks such as weak interaction with biomolecules or poor chemical stability. Recently explored 2D material, mixed metal carbides (MXenes) has unique properties such as large surface area, strong carrier confinement, incredible stability and hydrophillicity much better than other 2D materials [17]. In 2018, Wu et al. [18] compared the sensitivity of MXene based SPR sensor on using different metals, the highest sensitivity of 160°/RIU is achieved with Au-Mxene configuration. In 2019, Xu et al. [19] demonstrated highest sensitivityof198°/RIU for MXene and transition metal dichalcogenide based SPR sensor. Recently, in 2020, Pal et al. [20] used the BlueP/MoS_2 heterostructure with MXene and low refractive prism CaF_2 for enhancing the sensitivity up to 203°/RIU. Recently in 2021, Pandey et al. [21], theoretically investigated a SPR sensor based on heterojunction (MoO_3-$Ti_3C_2T_x$), which obtained the highest sensitivity (268.14°/RIU). For the further enhancement of the performance of the SPR sensor, the adherence composite layer of lower RI over the high RI material is used over the prism. The SiO_2 is used over the TiO_2 to make a composite layer. The light-trapping near the interface at the composite layer is enhanced due to the plasmon effect that enhances the surface plasmons (SPs), resulting in larger

resonance angle shift, which leads to advance the sensitivity of the SPR sensor [22]. In this paper, we proposed the 6-layer SPR sensor with constituent layers of $TiO_2/SiO_2/Au/Ti_3C_2T_x/SM$ over the low RI (BaF_2) prism. The proposed SPR sensor is theoretically and numerically analyzed at operating wavelength of 633 nm for RI range (1.330–1.355) of sensing medium.

This paper is prepared as follows. In Sect. 2, The sensor design consideration and the performance parameters are presented. In Sect. 3, the results are discussed under numerous sub-sections. To conclude the work presented here, finally the conclusion and required references are presented at the end.

2 Proposed Sensor Design

2.1 Design Consideration and Modeling

The schematic of the 6-layer proposed SPR sensor (Configuration: Prism BaF_2-TiO_2-SiO_2-Au-$Ti_3C_2T_x$-SM) is shown in Fig. 1. The first layer is the BaF_2 glass prism and its RI is $n_1 = 1.4733$ [21]. The second layer is TiO_2 and its RI $n_2 = 2.5837$ [23]. The third layer is SiO_2 and its RI is $n_3 = 1.4570$ [23]. The fourth layer is Au (gold) and its RI (n_4) is calculated from Eq. (1) as per the Drude model [10]. The fifth layer is $Ti_3C_2T_x$ and its RI is $n_5 = 2.38 + 1.33i$ [17]. The sixth layer is the sensing medium having RI of 1.33, which may vary up to 1.335 on adsorption of biomolecules. The thickness of Au and $Ti_3C_2T_x$ considered are 47 and, 0.993 nm with an optimized thickness of TiO_2 and SiO_2 (65–65 nm).

$$n = (\varepsilon_r + \varepsilon_i)^{\frac{1}{2}} = \left(1 - \frac{\lambda^2\lambda_c}{\lambda_p^2(\lambda_c + i\lambda)}\right)^{\frac{1}{2}} \tag{1}$$

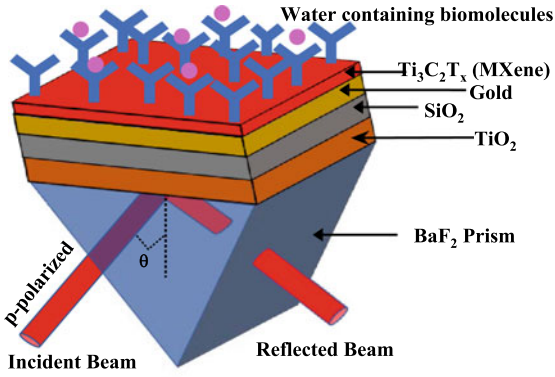

Fig. 1 Proposed SPR sensor

where collision and plasma wavelengths for Au are $\lambda_c = 8.9342 \times 10^{-6}$ m and $\lambda_p = 1.6826 \times 10^{-7}$ m respectively.

The reflectance of the p-polarized incident light is calculated using the transfer matrix method (TMM) as precise modeling with zero approximation [11]. The N-layer modeling is used for the calculation and systematic investigation of the reflectivity of the reflected light in the proposed SPR sensor. The mathematical modeling is described in our previous papers [11].

2.2 Performance Parameters of the SPR Sensor

Sensitivity is the ratio of a difference between two resonance angles ($\Delta\theta_{res} = \theta_2 - \theta_1$) to the RI shift of sensing layer ($\Delta n_s = 0.005$)

$$S = \frac{\Delta\theta_{\mathrm{Res}}}{\Delta n_s}(^{\mathrm{o}}/\mathrm{RIU}) \tag{2}$$

FWHM is change of resonance angles ($\theta_2 - \theta_1$) at 50% reflection intensity and measures the angular width of the SPR curve [24].

$$\mathrm{FWHM} = (\theta_2 - \theta_1) \tag{3}$$

DA is inversely proportional to the FWHM and given as:

$$DA = \frac{1}{FWHM}(1/^{\mathrm{o}}) \tag{4}$$

FoM is multiplication of the sensitivity and detection accuracy.

$$FoM = S \times DA(1/\mathrm{RIU}) \tag{5}$$

3 Discussion and Analysis of Numerical Results

First, we have optimized the thickness of the TiO_2-SiO_2 composite layer. The thickness of the TiO_2-SiO_2 has been optimized corresponding to reflectance and sensitivity with 47 nm of Au and monolayer of $Ti_3C_2T_x$ at 1.33 values of $n_{s,}$ shown in Fig. 2. In Fig. 2(a), it is clearly observed that the minimum reflectivity, Rmin. is reached at 65 nm thickness of both TiO_2 and SiO_2 layers. Similarly, at 65 nm of TiO_2 and $SiO_{2,}$ the maximum sensitivity 276°/RIU is obtained, shown in Fig. 2(b). Thus, the optimized thickness of TiO_2 and SiO_2 are 65 nm.

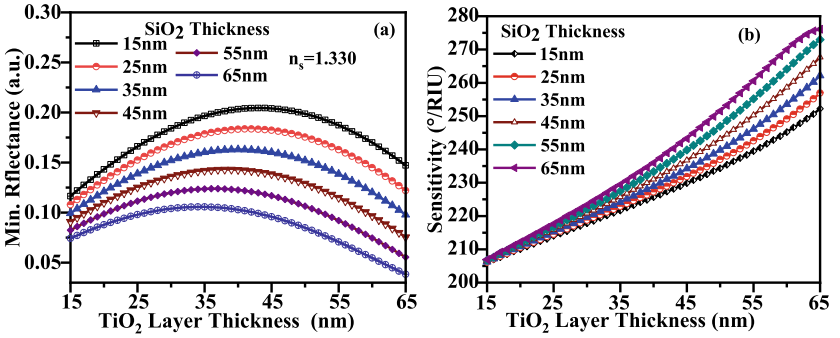

Fig. 2 TiO_2 and SiO_2 thickness optimization of in reference to **a** Min. reflectance and **b** sensitivity for Au (47 nm) and monolayerTi3C2Tx

The performance parameters of the sensor are calculated from the SPR characteristic curve illustrated in Fig. 3(a). The resonance angle shift, $\theta_{res.}$ due to alteration in RI of the sensing medium from 1.33 to 1.335, shown in Fig. 3(b). The performance parameters has been intended from SPR curves with $\Delta n_s = 0.005$. The sensitivity, FWHM, detection accuracy, and FoM are 276°/RIU, 12.02°, 0.083/° & 23/RIU, respectively. The Fig. 3(b) shows that the variation (shifting) in SPR curve in reference to alteration in sensing medium RI. From the Fig. 3(b) a linear variation in resonance angle is detected which varies from 80.2089° to 81.5891° corresponding to alteration the RI of sensing medium (1.330–1.335).

The performance parameter's analysis corresponding to the variation in RI of the sensing medium is presented, in Fig. 4. The maximum sensitivity 281.87°/RIU is achieved at 1.330 RI of the sensing medium then further it decreases from 281.87°/RIU to 276°/RIU with the alteration in RI of sensing medium (1.33–1.335), as per Fig. 4(a). In Fig. 4(a), the minimum reflectance increases from 3.84×10^{-2} to

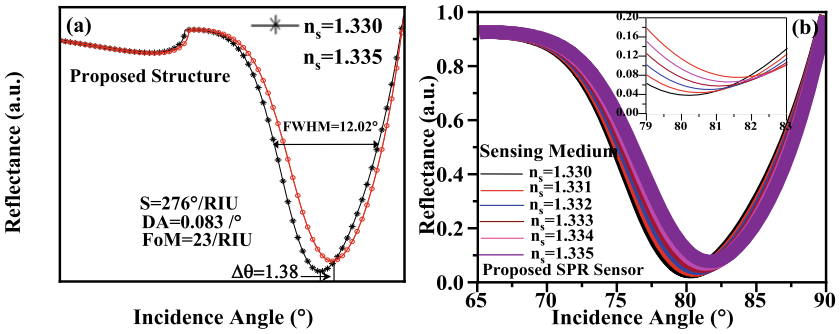

Fig. 3 **a** SPR reflectance curves of proposed SPR **b** Reflectance curve at various thickness of SiO_2 layer with 65 nm thickness of TiO_2 and monolayer of Ti3C2Tx and Au (47 nm)

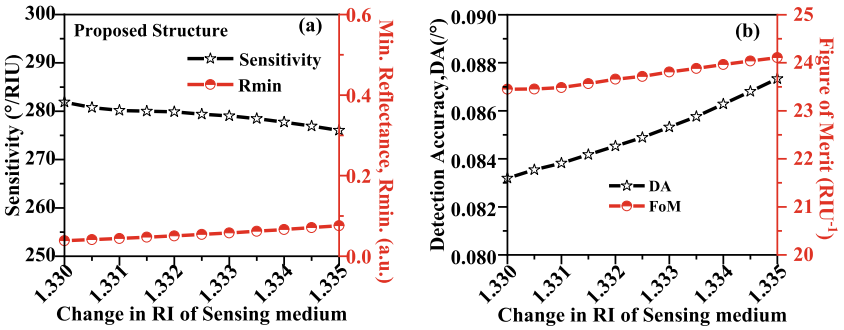

Fig. 4 **a** Sensitivity, Min. reflectance vs RI of sensing medium **b** Detection accuracy, FoM vs RI of sensing medium

7.95×10^{-2} a.u. with the increasing the RI (1.330 to 1.335) of the sensing medium due to increase in energy loss.

Figure 4(b) plot shows, the variation of detection accuracy and FoM with a slight modification in RI of the sensing medium. The FWHMs of the proposed SPR sensor are in decreasing manner, so its reciprocal, detection accuracy are increased from 0.0831/oto 0.0873/o. The overall performance of the SPR sensor is defined by FoM that is the product of sensitivity and detection accuracy. The FoM variations are from 23.450/RIU to 24.109/RIU corresponding to alteration in RI of sensing medium (1.330–1.335), respectively.

From Fig. 5, we can easily analyze the effect of the Mxene and composite layers on the SPR sensor. The Mxene based conventional SPR curves indicated by red colour demonstrates the more shifting of resonance angle as compared to conventional SPR due to improved adsorption of bio-molecules by the MXene, and change in resonance angle 0.967° is obtained. High real RI of TiO_2 gives large change in resonance angle up to 1.231° as compared to SiO_2, as shown in Fig. 5. For further upgrading the sensitivity of the sensor, we can introduce composite layers of TiO_2-SiO_2 which give the much larger change in resonance angle (1.38°) as compared to conventional SPR and SPR sensor without TiO_2 and SiO_2 layers.

Table 1 shows that the comparison between the proposed SPR sensor with the conventional SPR sensor as well as the proposed sensor with and without TiO_2 and SiO_2. From the Table 2, it is interpreted that the composite layer enhances the sensitivity as compare to conventional and rest of proposed SPR sensors due TiO_2 and SiO_2 enhancing the light trapping that enhance the plasmonic effect. The variation in the performance of the proposed SPR sensor corresponding to thickness variation in SiO_2 from 15 to 65 nm.

The COMSOL Multiphysics software is used for the analysis of the electric field enhancement by the finite element analysis (FEA) methods. The 1-D electric field distribution for the proposed SPR sensor within each layer is revealed in the Fig. 6(a). It is clear that, the TiO_2 and SiO_2 layer help to enhance the electric field at the interface of metal and composite layer and 2D material MXene also enhanced the electric

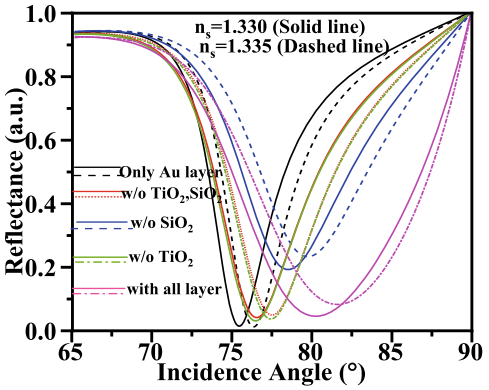

Fig. 5 SPR curves for the conventional SPR and proposed SPR with and without composite layer at ns = 1.330 and 1.335

Table 1 Performance parameters analysis with and without MXene, TiO_2 and SiO_2 layers

Structure layer	Δθ (deg.)	FWHM (1.33)	DA (deg^{-1})	S (°/RIU)	FoM (RIU^{-1})
Only Au layer	0.9	4.9	0.204	180	36.72
w/o TiO_2, SiO_2	0.967	6.73	0.148	193	28.56
w/o SiO_2	1.231	6.91	0.144	246	35.42
w/o TiO_2	0.955	6.83	0.146	191	27.88
With all layer	1.38	12.02	0.083	276	22.9

Table 2 Performance parameters with increasing the thickness of SiO_2 layer at 65 nm of TiO_2, monolayer of Au (47 nm) and $Ti_3C_2T_x$ (0.993 nm)

SiO_2 thickness	Δθ (deg.)	FWHM (1.33)	DA (deg^{-1})	S (°/RIU)	FoM (RIU^{-1})
15	1.26	7.92	0.126	252	31.75
25	1.28	8.66	0.115	257	29.55
35	1.31	9.46	0.105	262	27.51
45	1.34	10.31	0.096	268	25.72
55	1.37	11.17	0.089	273	24.29
65	1.38	12.02	0.083	276	22.9

field distribution interface of metal and MXene. The penetration depth of electric field in sensing medium is calculated from this 1-D electric field distribution. The penetration depth is 197 nm in the sensing medium for the proposed SPR configuration. The penetration depth of the SPR sensor is important parameter to build SPR with the molecule sized specific that immobilized at the surface. The range of penetration depth of conventional SPR is near to 100–250 nm with visible range of wavelength. The electric field intensity is plotted by the COMSOL Multiphysics

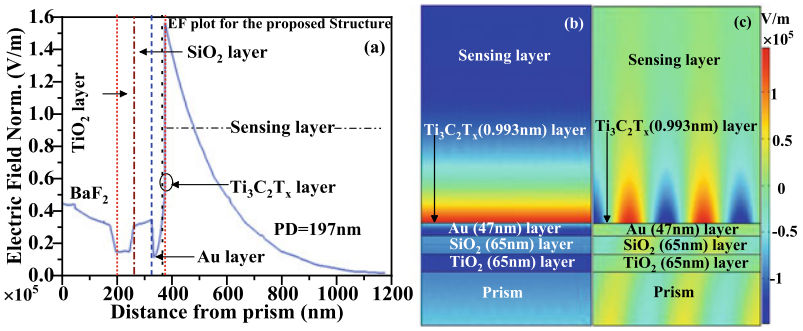

Fig. 6 **a** Electric filed distribution as a function of distance BaF2 to analyte **b** and **c** Field enhancement and SPs distribution at resonance state

Table 3 Comparison table of SPR sensors utilizing $Ti_3C_2T_x$, MXene

Structure	Sensitivity	References
BK7-Au-$Ti_3C_2T_x$	160	Wu et al. [18]
BK7-Au-TMD-Au-$Ti_3C_2T_x$	198	Xu et al. [19]
Prism-Metal-BlueP/MoS_2- $Ti_3C_2T_x$	203	Pal et al. [20]
SiO_2-Ag-MoO_3-$Ti_3C_2T_x$	268.14	A. K. Pandey [21]
BaF_2-TiO_2-SiO_2-Au-$Ti_3C_2T_x$	276	This work

as shown in Fig. 6(b and c). The electric field intensity is an important role in the SPR sensor. Figure 6(b and c) represents TM field distribution and SPs propagation respectively at various interface of the proposed sensor [BaF_2-TiO_2(65 nm)–SiO_2(65 nm)–Au(47 nm)-$Ti_3C_2T_x$(0.993 nm)-SM] w.r.t the normal distance from BaF_2 to sensing medium at resonance condition. The electric field enhancement in the y component at resonance angle is plotted in Fig. 6(b). The X–Y plane is considered as the TM-polarized incidence light. The mode coupling is responsible for E_y improvement at resonance state at 633 nm wavelength.

Table 3 is presented to compare proposed sensor with recent works for achieving maximum sensitivity. The work proposed here is capable to conquer the maximum sensitivity at 633 nm wavelength for ns = 1.330 and Δns = 0.005.

4 Conclusion

The proposed work is theoretically presented of an SPR sensor using a composite layer (TiO_2-SiO_2) with a monolayer of $Ti_3C_2T_x$ and Au. After adding the composite layer, the sensitivity is improved. It demonstrates the great sensitivity of 276°/RIU as compared to existing SPR sensor. The performance parameter is calculated at optimized TiO_2 and SiO_2 layer thicknesses at 65 nm with 47 nm of Au thickness.

It is further analyzed that on using the $Ti_3C_2T_x$ layer over Au layer, the sensitivity is enhanced. The penetration depth is 197 nm has been analyzed by the normalized electric field distribution. The proposed SPR sensor can be used for the field of medical and environmental science.

References

1. Sun, Y., Cai, H., Qiao, X., Wang, X.: High-performance polarization control modulated surface plasmon resonance sensor based on monolayer graphene/Au-NPs architecture for detection of DNA hybridization. Meas. Sci. Technol. **30**(12), 125701 (2019)
2. Arwin, H., Poksinski, M., Johansen, K.: Total internal reflection ellipsometry: principles and applications. Appl. Opt. **43**, 3028 (2004)
3. Caruso, F., Rodda, E., Furlong, D.N., Niikura, K., Okahata, Y.: Quartz crystal microbalance study of DNA immobilization and hybridization for nucleic Acid sensor development. Anal. Chem. **69**, 2043–2049 (1997)
4. Kukkar, M., Mohanta, G.C., Tuteja, S.K., Kumar, P., Bhadwal, A.S., Samaddar, P., Kim, K.-H., Deep, A.: A comprehensive review on nano-molybdenum disulfide/DNA interfaces as emerging biosensing platforms. Biosens. Bioelectron. **107**, 244–258 (2018)
5. Bayraç, C., Eyidoğan, F., AvniÖktem, H.: DNA aptamer based colorimetric detection platform for Salmonella Enteritidis. Biosens. Bioelectron. **98**, 22–28 (2017)
6. Xie, N., Huang, J., Yang, X., He, X., Liu, J., Huang, J., Fang, H., Wang, K.: Scallop-inspired DNA nanomachine: a ratio metric nano thermometer for intracellular temperature sensing. Anal. Chem. **89**, 12115–12122 (2017)
7. Basak, C., Hosain, M.K., Sazzad, A.A.: Design and simulation of a high sensitive surface plasmon resonance biosensor for detection of biomolecules. Sensing Imaging **21**(1), 2 (2020)
8. Miyoshi, H., Suehiro, N., Tomoo, K., Muto, S., Takahashi, T., Tsukamoto, T., Ohmori, T., Natsuaki, T.: Binding analyses for the interaction between plant virus genome-linked protein (VPg) and plant translational initiation factors. Biochimie **88**(3–4), 329–340 (2006)
9. Hossain, M., Rana, M.: DNA hybridization detection based on resonance frequency readout in graphene on Au SPR biosensor. J. Sens. (2016)
10. Singh, M.K., Pal, S., Prajapati, Y.K., Saini, J.P.: Highly sensitive antimonene based SPR biosensor for miRNA detection. Mater. Today Proc. **28**, 1776–1780 (2020)
11. Singh, M.K., Pal, S., Verma, A., Prajapati, Y.K., Saini, J.P.: Highly sensitive antimonene-coated black phosphorous-based surface plasmon-resonance biosensor for DNA hybridization: design and numerical analysis. J. Nanophotonics **14**(4), 046015 (2020)
12. Hasib, M.H.H., Nur, J.N., Rizal, C., Shushama, K.N.: Improved transition metal dichalcogenides-based surface plasmon resonance biosensors. Condensed Matter. **4**(2), 49 (2019)
13. Zhu, J., Ke, Y., Dai, J., You, Q., Wu, L., Li, J., Guo, J., Xiang, Y., Dai, X.: Topological insulator overlayer to enhance the sensitivity and detection limit of surface plasmon resonance sensor. Nanophotonics (2019)
14. Moznuzzaman, M., Islam, M.R., Hossain, M.B., Mehedi, I.M.: Modeling of highly improved SPR sensor for formalin detection. Results Phys. **16**, 102874 (2020)
15. Pal, S., Verma, A., Prajapati, Y.K., Saini, J.P.: Sensitive detection using heterostructure of black phosphorus, transition metal di-chalcogenides and MXene in SPR sensor. Appl. Phys. A **126**(10) (2020). https://doi.org/10.1007/s00339-020-03998-1
16. Xue, T., Liang, W., Li, Y., Sun, Y., Xiang, Y., Zhang, Y., Bao, Q.: Ultrasensitive detection of miRNA with an antimonene-based surface plasmon resonance sensor. Nature Commun. **10**(1) (2019). https://doi.org/10.1038/s41467-018-07947-8
17. Kumar, R., Pal, S., Prajapati, Y.K., Saini, J.P.: Sensitivity enhancement of MXene based SPR sensor using silicon: theoretical analysis. SILICON **13**(6), 1887–1894 (2021)

18. Wu, L., You, Q., Shan, Y., Gan, S., Zhao, Y., Dai, X., Xiang, Y.: Few-layer $Ti_3C_2T_x$ MXene: a promising surface plasmon resonance biosensing material to enhance the sensitivity. Sens. Actuators B Chem. **277**, 210–215 (2018)
19. Xu, Y., Ang, Y.S., Wu, L., Ag, L.K.: High sensitivity surface plasmon resonance sensor based on two-dimensional MXene and transition metal dichalcogenide: a theoretical study. Nanomaterials **9**(2), 165 (2019)
20. Pal, S., Pal, N., Prajapati, Y.K., Saini, J.P.: Sensitivity analysis of surface Plasmon resonance biosensor based on Heterostructure of 2D BlueP/MoS_2 and MXene. In: Inamuddin, B.R., Ahamed, M.I., Asiri, A.M. (eds.) Layered 2D Advanced Materials and Their Allied Applications, pp. 103–129. Wiley (2020) https://doi.org/10.1002/9781119655190.ch5
21. Pandey, A.K., Hashemi, M.: Plasmonic sensor based on molybdenum trioxide-MXene heterojunction for refractive index sensing. Arab. J. Sci. Eng. 1–6 (2021)
22. Xu, J., Xiao, X., Stepanov, A.L., Ren, F., Wu, W., Cai, G., Zhang, S., Dai, Z., Mei, F., Jiang, C.: Efficiency enhancements in Ag nanoparticles-SiO_2–TiO_2 sandwiched structure via plasmonic effect-enhanced light capturing. Nanoscale Res. Lett. **8**, 73 (2013)
23. Maurya, J.B., Prajapati, Y.K., Singh, V., Saini, J.P.: Sensitivity enhancement of surface plasmon resonance sensor based on graphene–MoS_2 hybrid structure with TiO_2–SiO_2 composite layer. Appl. Phys. A **121**(2), 525–533 (2015)
24. Maurya, J.B., Prajapati, Y.K.: A novel method to calculate beam width of SPR reflectance curve: a comparative analysis. IEEE Sens. Lett. **1**(4), 1–4 (2017)